

# Mangosteen Peel-Alginate Biocomposite Beads An Efficient and Sustainable Adsorbent For Decontamination of Methylene Blue

Asma Nasrullah (✉ [advent\\_chemist@yahoo.com](mailto:advent_chemist@yahoo.com))

Technology University of Petronas: Universiti Teknologi PETRONAS

Amir Sada Khan

University of Science and Tecnology Bannu

A. H. Bhat

Higher Colleges of Technology

Taghreed M. Fagieh

King Abdulaziz University

Ersaa M. Bakhsh

King Abdulaziz University

Kalsoom Akhtar

king abdulaziz

Sher Bahadar khan

King Abdulaziz University

Israf Ud Din

Prince Sattam bin Abdulaziz University

Shahan Zeb Khan

University of Science and Tecnology Bannu

---

## Research Article

**Keywords:** Mangosteen peel waste, methylene blue, kinetic study, alginate beads, isotherm study

**Posted Date:** November 2nd, 2021

**DOI:** <https://doi.org/10.21203/rs.3.rs-1038092/v1>

**License:**   This work is licensed under a Creative Commons Attribution 4.0 International License.

[Read Full License](#)

---

1 **Mangosteen peel-alginate biocomposite beads an efficient and sustainable adsorbent for**  
2 **decontamination of methylene blue**

3 Asma Nasrullah<sup>a,b\*</sup>, Amir Sada Khan<sup>c</sup>, A. H. Bhat<sup>d</sup>, Taghreed M. Fagieh<sup>e</sup>, Esraa M. Bakhsh<sup>e</sup>,  
4 Kalsoom Akhtar<sup>e</sup>, Sher Bahadar Khan<sup>e,f</sup>, Israf Ud Din<sup>g</sup>, Shahan Zeb<sup>h</sup>

5 <sup>a</sup>Fundamental and Applied Sciences Department, Universiti Teknologi PETRONAS (UTP),  
6 32610 Bandar Seri Iskandar, Perak, Malaysia

7 <sup>b</sup>National Centre of Excellence in Physical Chemistry, University of Peshawar, Peshawar  
8 25120, Pakistan

9 <sup>c</sup>Department of Chemistry, University of Science & Technology, Bannu 28100, Khyber  
10 Pakhtunkhwa, Pakistan

11 <sup>d</sup>Department of Applied Science, Higher College of Technology, Muscat- 133, Oman

12 <sup>e</sup>Department of Chemistry, Faculty of Science, King Abdulaziz University, P.O. Box 80203,  
13 Jeddah 21589, Saudi Arabia

14 <sup>f</sup>Center of Excellence for Advanced Materials, King Abdulaziz University, P.O. Box 80203,  
15 Jeddah 21589, Saudi Arabia

16 <sup>g</sup>Department of Chemistry, College of Science and Humanities, Prince Sattam Bin Abdulaziz  
17 University, P.O. Box 173, Al-Kharj, Saudi Arabia

18 Pakistan **Corresponding authors email:** advent\_chemist@yahoo.com

19 **Abstract**

20 This study examines mangosteen peels waste and alginate beads (MPAB) as an efficient,  
21 sustainable and low-cost adsorbent for removal of methylene blue (MB) cationic dye from  
22 aqueous solution in a batch adsorption system. Surface functional groups, surface morphology,  
23 surface properties, and thermal stability of MBAB were analyzed using various instrumental  
24 techniques such as FTIR, FESEM, BET and TGA techniques. MPAB adsorption efficiency for  
25 MB was investigated through variation of dosage (0.01- 0.08g), pH (2- 10), contact time (60-  
26 1320 min), MB concentration (20- 100 mg/L) and temperature (298- 333K). MPAB showed  
27 maximum removal capacity of 373 mg/g at 25 °C in basic medium. Kinetic and isotherm studies  
28 showed that pseudo second order kinetic models and both Freundlich and Langmuir isotherms  
29 best fit the experimental data. The findings revealed that novel MPAB has the potential to be a  
30 cost-effective adsorbent for removal of textile dyes.

31 **Keywords:** Mangosteen peel waste; methylene blue; kinetic study; alginate beads; isotherm  
32 study

## 35 1. Introduction

36 In this modern day and age, novel dyes treatment technologies are required which can  
37 remove dyes from wastewater as well as reduce the potential toxicity to humans and the  
38 ecosystem [1]. Various types of technologies such as adsorption, membrane separation,  
39 coagulation, electrochemical, biological and adsorption are frequently used for wastewater  
40 containing dyes [2]. Among the various available method, adsorption is frequently used for  
41 decolorization of dye-containing water because of adsorption's economic and efficacious, and  
42 advantages. Different types of adsorbents such as activated carbon [3], geopolymer [4], clay  
43 minerals [5], industrial and agricultural wastes [6], zeolites [7] can be efficiently utilized in an  
44 adsorption process. However, these adsorbents have some disadvantages such as poor  
45 adsorption capacity and high cost [8].

46 Low-cost adsorbents require that the precursor be non-hazardous, easily accessible and  
47 relatively cheap. Much attention and interest have been increasing in using attractive, cheaper  
48 alternatives for decolorizing dye-contaminated water. In general, an adsorbent can be assumed  
49 to be "low cost" if it is freely available, requires little processing (such as by being a by-  
50 product), or is an industrial waste material that has lost its economic or further processing  
51 values. Indeed, the use of free biomass (industrial waste product or agricultural waste material)  
52 for the treatment of dyes through adsorption is a successful method. Biomass powder can  
53 effectively adsorb dyes due to high surface area; However, due to weak mechanical properties,  
54 low rigidity, high steric hindrance, high packing density and hydraulic conductivity, the powder  
55 form is not considered appropriate for column-type filtration [9]. Moreover, the powder  
56 biomass adsorbents are not easily recyclable and reusable. Due to the above mentioned  
57 disadvantages, the extensive use of powdered biomass or other agricultural adsorbents becomes  
58 narrowed due to process engineering difficulties such as reactor clogging, dispersion, and cost  
59 of regeneration [10, 11].

60 An alternate way exists to entrap the powder adsorbent in other supporting material,  
61 resulting in a new class of adsorbent. The utilization of alginate as a carrier substance for  
62 powdered adsorbent allows for the possibility of selective adsorption of dye molecules,  
63 depending upon the carrier charge, which interact with negative charge of carboxylate groups  
64 on alginate. Alginate is most commonly used because of its low cost, biodegradation, and  
65 ability to readily transform into hydrogels in aqueous solution [12]. Researchers have  
66 previously used Ca-alginate based adsorbent beads successfully to adsorb MB dye from  
67 aqueous solution [12-15]. Several studies has been conducted to entrap carbonaceous material  
68 such as activated carbon (AC) [16], multiwall-carbon nanotubes (MWCN) [17-19], graphene

69 oxide (GO) [20], ash [21], graphite nanocarbon (GNT) [22] and lignocellulosic biomass [23,  
70 24] into biopolymer beads alginate [25]. However, AC, MWCN, GO, ash and GNT have  
71 complex synthesis process and, therefore, less economic viability on an industrial scale.

72         Among available lignocellulosic biomass, mangosteen, botanical name *Garcinia*  
73 *mangostana*, belongs to the family Clusiaceae and genus *Garcinia*. Mangosteen gives fruit  
74 which contains 25-30% edible part and the remaining 60-75% is a dark or light purple color  
75 peel [26] . Mangosteen trees are most abundantly grown in South East Asian countries such as  
76 Thailand, Malaysia and Indonesia [27] . It has a nice taste, can be eaten fresh, and can be used  
77 to produce wine, jam, preserves and puree. It has extensive medicinal value and used in  
78 treatment wound healing, diarrhea, fever, eczema and many other diseases. The Malaysian  
79 Ministry of Agricultural and Agro based industry has stated that 1 kilo of mangosteen fruit can  
80 produce about 0.6 Kg of MP waste[28], which is renewable, easily accessible, and relatively  
81 inexpensive. This MP waste can be used as adsorbent in various forms (powder, beads, and  
82 membranes) [16, 29, 30]. Problems associated with MP includes improper disposal and  
83 burning in open atmosphere, which can create environmental problems. Recent literature has  
84 shown that MP and MP based adsorbents efficiently remove methylene blue (MB) dye from  
85 aqueous media. With a higher adsorption efficiency, MP and MP-based adsorbents can be used  
86 as a low cost, efficient and easily available material for adsorption purpose. However, the MP  
87 powder is not suitable from an engineering point of view because of regeneration and  
88 recyclability issues. Therefore, its encouraged to use powder in the form of beads or membrane  
89 for dye extraction from water stream because of ease regeneration and recyclability.

90         To the best of our information, no previous literature that addresses MP powder in  
91 alginate for MB dye removal exist. The main goal of this research work was to synthesize  
92 mangosteen peel-alginate beads (MPAB) for efficient removal of MB dye from aqueous  
93 solution. MPAB were systematically characterized using BET surface area analysis, SEM,  
94 TGA and FT-IR. Process parameters, such initial pH of MB solution, MPAB dose, contact  
95 time, initial concentration of MB, and temperature, were studied and optimized. To find the  
96 feasibility and spontaneity of the adsorption process, theoretical studies of adsorption kinetics,  
97 adsorption isotherms, and thermodynamics were performed.

## 98     **2. Experimental**

### 99     **2.1 Materials**

100         AC prepared from MP waste was used. All chemicals used in this research work were  
101 used without any further processing. Methylene blue, HCl and NaOH were purchased from

102 R&M chemical, and  $\text{CaCl}_2$  was purchased from Merck Germany. Sodium alginate (Mol. Wt.  
103 120,000-190,000 g/mol, viscosity 15-25cP, 1% in  $\text{H}_2\text{O}$ ) was purchased from Sigma-Aldrich.

## 104 **2.2 Preparation of MPAB**

105 The MP-alginate beads were synthesized from MP powder mixed with sodium alginate  
106 in a 2:1 ratio in distilled water. The MP powder and Na-alginate were mixed thoroughly in a  
107 petri dish and then slowly added to the distilled water in many steps. The slurry of MP and  
108 alginate was stirred at 400 rpm for 5 h, which resulted in a clear solution. The slurry was then  
109 sonicated for 30 min to remove the trapped bubbles present in slurry. The slurry was added  
110 dropwise to the 5% solution of  $\text{CaCl}_2$  which resulted in the synthesis of spherical gel MPAB  
111 via cross linking. To ensure complete cross linking, the MPAB beads were stirred for 24h in  
112 cross linker solution. After 24h of this cross-linking process, the beads were removed from the  
113  $\text{CaCl}_2$  solution and washed with excess deionized water to ensure that no  $\text{CaCl}_2$  molecules were  
114 left over on the MPAB surface. The synthesized MPAB was dried in an oven at  $60^\circ\text{C}$ . The  
115 average size of MPAB was approximately 1.30 mm. The synthesized beads were placed in air  
116 sealed glass bottle and used for adsorption study of MB. **Figure 1** shows photograph of  
117 synthesized MPAB.

118 **Fig. 1.**

## 119 **2.3 Characterization of the MPAB**

120 The synthesized materials can be characterized by using different types of instruments  
121 before its targeted adsorbent application. These various material surface properties help to  
122 explain the adsorption data. Surface properties of MPAB were measured using a surface area  
123 and pore size analyzer (Micromeritics ASAP 2020) with  $150^\circ\text{C}$  degassing temperature for 6 h.  
124 FTIR (Perkin, Elmer, Frontier) was used to identify surface active/functional groups available  
125 on the surface of MPAB before and after adsorption. FTIR spectra of the beads were  
126 measured in the region with range from  $4000$  to  $400\text{ cm}^{-1}$  in inert atmosphere by mixing the  
127 beads with KBr pellet. SEM (Zeiss Supra55 VP) was used to study surface morphology of  
128 synthesized MPAB. Thermal stability of beads was measured using a Perkin Elmer, ASTA 6000  
129 thermogravimetric analyzer (TGA) in inert atmosphere of nitrogen with a temperature range  
130 from  $50$  to  $800^\circ\text{C}$  and a  $10^\circ\text{C}/\text{min}$  heating rate.

## 131 **2.4 Batch adsorption tests**

132 To calculate the adsorption efficiency, the adsorption efficiency of beads were  
133 performed under different experimental conditions. A predetermined amount of beads were  
134 added to 20mL MB solution having specific concentration under room temperature. The flask

135 was placed in orbital shaker and was shaken at 150 rpm. At completion of each specific  
 136 adsorption experiment, about 2 mL of MB solution was taken out from the flask with a syringe  
 137 and put into a UV-Vis vial. The vial was placed in UV-Vis spectrophotometer for measurement  
 138 of MB concentration. The concentration of MB in bulk solution was determined by a UV-Vis  
 139 spectrophotometer (Shimadzu 1800) at 664 nm using standard MB curve with the regression  
 140 coefficient of the standard plot 0.998. The percentage removal (% R), adsorption capacity ( $q_t$ )  
 141 and adsorption capacity at equilibrium were measured using the below equations [31]:

$$\%R = \left( \frac{C_i - C_f}{C_i} \right) \times 100 \quad (1)$$

$$q_t = \left( \frac{C_i - C_f}{m} \right) \times V \quad (2)$$

$$q_e = \left( \frac{C_i - C_f}{m} \right) \times V \quad (3)$$

142 Where  $C_i$  and  $C_f$  ( $\text{mg.L}^{-1}$ ) is the initial and final MB concentration,  $m$  (g) is the mass of  
 143 adsorbent and  $V$  (L) is the volume of MB solution used in the adsorption experiments. To  
 144 ensure maximum adsorption capacity of beads for MB adsorption, the effect of process  
 145 parameters such as pH of initial MB solution (2-10), adsorbent dose (0.01-0.08g), contact time  
 146 (60-1320 min), initial MB concentration (20-100 mg/L), and temperature (298.15-333.15K)  
 147 were studied and optimized. The beads were recycled and reused by using a solution of NaCl  
 148 (0.5M) and methanol mixed in the same volume ratio. The beads were recycled and reused five  
 149 times. The desorption was calculated by the following formula:

$$\% \text{ Desorption} = \frac{\text{Mass of desorbed MB}}{\text{Mass of adsorb MB}} \times 100 \quad (4)$$

## 150 2.5 Theoretical study

151 To better understand bead MB adsorption, kinetic, isotherm and thermodynamic studies  
 152 were performed. For kinetic study of adsorption of MB on MPAB beads, a predetermined  
 153 amount of beads was mixed with a specific amount of MB solution with a concentration in a  
 154 range from 20 ppm to 100 ppm and was shaken for varying intervals of time, ranging from 60  
 155 min to 1320 min. The experimental data for MB adsorption on beads was procured by using  
 156 two well-known pseudo-first order (PFO) [32] and pseudo-second order (PSO) [33] kinetic  
 157 models. During the isotherm study, the adsorption experiments were run at different  
 158 concentrations of MB solution in a range from 20 mg/L to 100 mg/L under optimized  
 159 conditions until equilibrium was reached. The equilibrium data obtained in this study for the  
 160 removal of MB on MPAB were analysed using four well kown adsorption isotherms models:

161 Langmuir [34], Freundlich [35] Tempkin [36] and Harkins-Juar [37]. To study the  
162 thermodynamics of adsorption of MB on MP-alginate beads, MPAB mixed with MB solution  
163 were run at various temperatures ranging from 298.15 to 333.15 K under optimized  
164 experimental conditions. Changes in various thermodynamic parameters such as enthalpy  
165 ( $\Delta H$ ), entropy ( $\Delta S$ ) and Gibbs free energy ( $\Delta G$ ) for MB adsorption on MPAB were calculated  
166 in order to examine the spontaneity of a process.

### 167 **3. Results and Discussion**

#### 168 **3.1. Physical Characterization of MPAB**

##### 169 **3.1.1. FTIR study**

170 The active groups present on the MPAB surface were analyzed using FTIR analysis.  
171 **Figure 2.** shows the FTIR spectra of MPAB before and after MB adsorption. The peaks  
172 appeared at  $3419\text{ cm}^{-1}$  (O-H group stretching),  $2927\text{ cm}^{-1}$  (aliphatic C-H stretching vibration),  
173  $1613\text{ cm}^{-1}$  (C=O stretching vibration) and at  $1036\text{ cm}^{-1}$  (-OH alcoholic) [38]. After MB  
174 adsorption, the stretching vibration of peaks -OH and -C=O groups due to intermolecular  
175 hydrogen-bonding with MB molecule are shifted from  $3419$  to  $3412\text{ cm}^{-1}$  and from  $1627$  to  
176  $1613\text{ cm}^{-1}$ , respectively. Similar adsorption phenomena for MB on alginate beads have already  
177 been reported in literature [8, 39]. Owing to electrostatic attraction between MB and MPAB,  
178 the intensity of peaks located at  $1613\text{ cm}^{-1}$  and  $1036\text{ cm}^{-1}$  is considerably decreased [8]. An  
179 oxygen containing functional group has a peak at  $1437\text{ cm}^{-1}$ , corresponding to stretching  
180 vibration of  $\text{-COO}^-$ , considerable decrease in intensity after MB adsorption. This decrease in  
181 intensity is due to the extinction of some of  $\text{-COO}^-$  groups involved in MB molecules  
182 adsorption [40, 41]. MB and others cationic dyes due to planner structure can be easily  
183 adsorbed on the adsorbent surface by van der Waals forces. The FTIR analysis confirmed that  
184 MPAB contain a large number of hydroxyl and carbonyl groups, which are considered active  
185 interaction sites that interact with MB and others cationic dyes.

#### 186 **Fig. 2**

##### 187 **3.1.2 Morphology of MPAB**

188 FESEM technique was used to determine morphological properties and surface features  
189 of MPAB. **Figure 3** shows the FESEM micrographs of MPAB taken under different  
190 magnifications. The FESEM photographs show that the composite beads of MP-alginate have  
191 a rough surface that contains numerous bulges and cracks. Generally, the surface observed in  
192 this study are very common and observed by others researchers of alginate beads [38, 39].

193 To study the surface porosity such as surface area and pore sizes of MPAB, N<sub>2</sub>  
194 adsorption-desorption for MPAB were performed. N<sub>2</sub> adsorption-desorption isotherm for  
195 MPAB is shown in **Figure 4a**. The BET result indicated that beads follow type IV adsorption-  
196 desorption isotherm, showing mesoporous (2-50 nm) nature of synthesized beads [42]. The  
197 hysteresis loop also suggests that the MPAB beads are mesoporous in nature, with a pore  
198 diameter in the range of mesoporous according to IUPAC classification [43]. The BET surface  
199 area and Langmuir surface area for MP-alginate beads was 0.725 m<sup>2</sup>/g and 1.26 m<sup>2</sup>/g,  
200 respectively. An adsorbent's having a mesoporous structure is consider good to adsorb large  
201 molecules of various types of dyes, proteins, and polycyclic aromatic compounds [10].

### 202 **3.1.3 TGA analysis**

203 TGA was used to investigate the thermal decomposition behavior of MP powder and  
204 MP immobilized in alginate beads. Thermal properties of MP and MPAB measured in the  
205 temperature range of 50 - 850 °C are shown in **Figure 4b**. The small weight loss in both samples  
206 below 105 °C is due to vaporization of volatile organic compounds and moisture attached on  
207 the surface of MP and MPAB surface. The samples of both MP and MPAB are stable below  
208 190 °C [44, 45].. The TGA curve shows one predominant weight loss and major degradation  
209 occurring in region from 190 °C to 360 °C [20, 21]. Thermal degradation of MPAB in this  
210 region might be due to the loss of water vapors trapped inside the beads [46]. The result  
211 demonstrated that the MPAB is thermally more stable than MP powder at all temperatures  
212 except in the temperature range from 190 to 320 °C. In the second stage, the maximum thermal  
213 degradation of both samples takes place. This major thermal degradation is due to degradation  
214 of cellulose and hemicellulose present in both samples [1]. It seems that alginate cause increase  
215 in thermally stability of MP. Vecino et al. [47] also observed same trend of TGA for vineyard  
216 pruning waste immobilized in alginate and found that these beads are thermally stable below  
217 200 °C. Sargin et al. [48] also noticed an increase in thermal stability of microfungus spores  
218 composite beads.

219 **Fig. 4**

## 220 **3.2. Adsorption Study**

### 221 **3.2.1. Adsorbent dose effect**

222 MB adsorption as function of MPAB dose (0.01- 0.08 g) is represented in **Figure 5a**.  
223 The adsorption experiment was run for 60 min using pH 10. It was discovered that the  
224 adsorption capacity of beads for MB decreased from 137 to 22 mg/g while % R increase from  
225 68.62 to 87.7% with the increase of MPAB. However, the decrease in adsorption capacity  
226 might be due to availability, or lack thereof, of free active sites after adsorption of all dye's

227 molecules and an inverse relation between adsorption capacity and adsorption dose, as shown  
228 in Eqn. 2. The increase in %R of MB with increase of adsorption dose is due to migration of  
229 many molecules from liquid phase to solid phase. The findings are very common and similar  
230 findings are reported elsewhere in literature [49].

### 231 **3.2.2 pH effect**

232 Initial pH of MB solution plays a very key role in adsorption, and therefore it is a  
233 priority to understand the effect of pH on MPAB adsorption. The pH of MB solution was varied  
234 from 2 to 10. Effect of initial pH of MB solution on beads performance is shown in **Figure 5b**.  
235 Results, provided in Figure 6, clearly indicate that adsorption efficiency of beads for MB is  
236 greatly affected by pH. The adsorption of dye on the surface of adsorbents occurs due to  
237 electrostatic attraction that exists between MB cation and a negatively charged presence on  
238 adsorbent surface. Initial pH of MB solution has considerable effect on MB removal. The  
239 adsorption capacity of MB on MPAB jumps from 141.5 to 182 mg/g when pH of solution  
240 increases from 2 to 10. In acidic pH region (below pH 6), the low adsorption efficiency of  
241 MPAB for MB dye adsorption is due to the competition of H<sup>+</sup> ions and MB molecules to bind  
242 with active sites. However, with an increase of pH from acidic to basic region (above pH 7),  
243 the adsorption capacity considerably increases. The highest adsorption capacity was noted at  
244 pH 9.5. This increase in adsorption efficiency is due to the increase in negative charge on the  
245 surface of MPAB. This increase in negative charge on the adsorbent surface can increase the  
246 interaction of MB cations with the surface of MPAB. However, the uptake of MB slightly  
247 increases with the increase of pH of solution greater than 8. Therefore, initial pH of MB  
248 solution was selected as 9.5. The removal capacity of MB dye on various types of adsorbents  
249 in a basic pH range has already been reported in literature elsewhere [50]. Maximum adsorption  
250 of MB for alginate/activated carbon was observed at pH 10 [38].

### 251 **3.2.3 Initial concentrations and contact time effect**

252 To optimize adsorption conditions for dye removal from aqueous phase to solid phase,  
253 the study of contact time and solution concentration is considered crucial. The effect of initial  
254 MB concentration (20 - 100 mg/g) and contact time (60-1320 min) on adsorption efficiency of  
255 MPAB (pH 9.5, adsorbent dose 0.01 g and 25 °C) is shown in **Figure 5c**. The results confirmed  
256 the quick adsorption of MB dye occurred early in time. High adsorption efficiency at initial  
257 contact time is fast due to high mass transfer and rapid approach of MB cations to the surface  
258 of MPAB and coverage of more active sites with cations of dye at early stage. However, as  
259 contact time increases, elimination of MB from aqueous solution decreases due to the

260 saturation of active sites of adsorbent with dye molecules. The adsorption capacity of MB on  
 261 MPAB is fast until 600 min and very small increase was observed after 1080 min. Zhuang et  
 262 al. [50] found a decrease in removal of MB dye on GO/alginate beads with higher contact time  
 263 between MB and beads, and equilibrium was achieved after 1200 min. The results in Figure 7  
 264 shows that the removal efficiency of beads for MB increases from 83 mg/g to 185 mg/g with  
 265 the increase of dye concentration from 20mg/g to 100 mg/g. This increase is due to the presence  
 266 of more MB cations in the solution that interact and bind with the active surface functional  
 267 groups of adsorbent surfaces. This increase in adsorption capacity of beads for MB is very  
 268 normal and is extensively reported by other researchers elsewhere [16, 51].

269 **Fig. 5**

### 270 **3.3 Kinetic Study for MB adsorption**

271 To study the kinetics of MB adsorption on MPAB, PFO (Eqn. 4) and PSO kinetic  
 272 models (Eqn. 5) were applied for the experimental data of MB on beads [32].

$$273 \log(q_e - q_t) = \log q_e - \frac{k_1}{2.303} \times t \quad (4)$$

274 where  $k_1$  is the pseudo first order rate constant and  $q_e$  and  $q_t$  ( $\text{mg.g}^{-1}$ ) are the amounts of MB  
 275 adsorbed at equilibrium and at time  $t$  (min), respectively. The plot of  $\log(q_e - q_t)$  gives the  
 values of  $q_e$  and  $k_1$ .

$$276 \frac{t}{q_t} = \frac{1}{k_2 q_e^2} + \frac{t}{q_e} \quad (5)$$

277 Where  $q_t$  ( $\text{mg/g}$ ) is the amount of adsorbed MB on MPAB at time  $t$  (min). The rate  
 278 constant  $k_2$  for pseudo second order model and  $q_e$  can be deduced from the intercept and slope  
 279 of the plot  $t/q_t$  and  $t$ . **Figure 6** shows the linear plots obtained for MB adsorption at various  
 280 times using PFO and PSO kinetic models while Table 1 shows the various kinetic parameters  
 281 obtained for MB adsorption. The value of  $R^2$  (0.997) shows that MB adsorption on MPAB is  
 282 well fit by pseudo second order kinetic model. In addition, the theoretical value of adsorption  
 283 capacity calculated for various concentration of MB removal on MPAB is close to the  
 284 experimental values. This close agreement between the experimental and theoretical values of  
 285 adsorption capacity supports that MB adsorption on MPAB is well fit by the PSO kinetic model  
 286 (**Figure 6b**). Khanday et. al. also observed that PSO kinetic model well described the MB  
 adsorption on activated palm oil ash/zeolite/chitosan beads [13].

287 **Fig. 6**

288 **Table 1.**

### 289 3.4 Adsorption isotherm study

290 The equilibrium data obtained in this study for MB adsorption on MPAB were analysed  
291 using Langmuir [34], Freundlich [35] Tempkin [36] and Harkins-Juar [37] isotherms. Linear  
292 form of Langmuir isotherm model is shown in Eqn. 6 as given below:

$$\frac{C_e}{q_e} = \frac{1}{bq_{max}} + \frac{1}{q_{max}} \times C_e \quad (6)$$

293 where  $C_e$  (mg/L) is MB concentration,  $q_{max}$  (mg/g) is maximum amount of dye adsorbed, and  
294  $b$  is referred as Langmuir constant. The slope and intercept of the plot of  $C_e/q_e$  and  $C_e$  gives  
295 the values of  $q_{max}$  and  $b$ , respectively. The empirical relationship of  $q_e$  and  $C_e$  is determined  
296 from the Freundlich isotherm model, which explains the heterogeneity of the system. Eqn. 7  
297 can explain the Freundlich isotherm model:

$$\ln q_e = \ln K_F + \frac{1}{n} \ln C_e \quad (7)$$

298 Where  $K_F$  and  $1/n$  are the Freundlich isotherms constants and represent adsorption capacity  
299 and intensity, respectively. The linear plot drawn for various adsorption isotherms is shown in  
300 Figure 9. Various thermodynamic parameters obtained from the linear plot of Freundlich and  
301 Langmuir adsorption isotherms are given in Table 2. The slope and the intercept of linear plot  
302 of  $\ln q_e$  versus  $\ln C_e$  give the values of both of  $n$  and  $K_F$ . The values of  $n$  and  $K_F$  are displayed in  
303 Table 2. The value of  $n$  for MB adsorption on beads is greater than 1, which confirm the  
304 convenient adsorption and heterogeneity of adsorption. The regression coefficients obtained for  
305 adsorption of MB using beads are relatively close to each other and greater than Tempkin and  
306 Harkin-Jura adsorption isotherms. The removal of MB on MPAB is fitted by both of the applied  
307 isotherm models, confirmed from the value of the correlation coefficient obtained ( $R^2$ ) for  
308 Langmuir (0.995) and Freundlich (0.989) isotherm models.

309 **Fig. 7**

310 **Table 2.**

### 311 3.5 Thermodynamic study

#### 312 3.5.1 Temperature effect

313 Temperature significantly affects the adsorption capacity of MPAB for MB dye. To  
314 find the effect of temperature on the removal efficiency of beads for MB, the adsorption  
315 experiments were performed under different temperatures ranging from 298.15 K to 333.45 K,  
316 using optimized experimental conditions. The temperature effect on MB adsorption on MPAB  
317 is displayed in **Figure 8a**. The capacity of adsorption of beads for MB removal at 298, 303,

318 313, 323 and 333 K were 185, 1801, 177, 166 and 151 mg/g, respectively. The result  
 319 demonstrated that an increase in temperature causes a decrease in the MB uptake from aqueous  
 320 solution. With an increase of temperature, dye molecules have a higher energy which might  
 321 cause a decrease in attraction with adsorbent surface. The decrease in adsorption capacity of  
 322 MB onto MPAB at higher temperature indicates the exothermic nature of the adsorption.  
 323 Thermodynamic parameters calculated for MB removal by MPAB can be determined by  
 324 performing adsorption experiments under various temperatures. Eqn. 12 was used for  
 325 calculation of Gibbs free energy. Other thermodynamic parameters, such as entropy and  
 326 enthalpy for adsorption process, can be calculated by plotting  $\ln K_c$  versus  $1/T$  using Eqn. 13.  
 327 **(Figure 8b).**

$$328 \quad K_c = \frac{q_e}{C_e} \quad (11)$$

$$329 \quad \Delta G^0 = -RT \ln K_c \quad (12)$$

$$330 \quad \ln K_c = \frac{\Delta S^0}{R} - \frac{\Delta H^0}{RT} \quad (13)$$

331 Where T is the absolute temperature in K,  $K_c$  is the equilibrium constant and R is the  
 332 general gas constant ( $8.314 \text{ J} \cdot \text{mol}^{-1} \cdot \text{K}^{-1}$ ). The calculated values of Gibbs free energy were -7.93,  
 333 -7.36, -7.14, -6.08 and -5.06 KJ/mol at 298, 303, 313, 323 and 333 K, respectively (**Table 3**).  
 334 The negative value of  $\Delta G^0$  revealed the spontaneity of adsorption process. The chemical or  
 335 physical nature of adsorption of MB can be determined by the value of  $\Delta G^0$ . The value of  $\Delta G^0$   
 336 in the range of -20 KJ/mol to 0 KJ/mol, indicated the physical nature of MB adsorption on  
 337 beads. The -ve values of  $\Delta S^0$  and  $\Delta H^0$  gives information that the adsorption of MB on MPAB  
 338 is spontaneous and exothermic [52]. The negative  $\Delta S^0$  value indicate the decrease in  
 339 randomness at MPAB interface as a result of MB adsorption [24, 38].

340 **Fig. 8**

341 **Table 3.**

### 342 **3.6 Recyclability and reusability of beads**

343 The worth of an adsorbent in industrial use is increased if said adsorbent is recyclable  
 344 and reusable. The adsorbents were recycled and reused five times without any considerable  
 345 decrease in adsorption efficiency. The first five adsorption capacities for beads were 95%, 92%,  
 346 90%, 85% and 80%, respectively. This finding confirmed that our synthesized beads are easily  
 347 recyclable and reusable, which decreases the capital cost of the process.

348

349

### 350 **3.7 Comparison with other beads**

351 Several adsorbents have been reported in the literature for MB adsorption from aqueous  
352 solution. **Table 4.** shows comparison of the MPAB with alginate beads already reported in  
353 literature [15, 20, 53-60]. The results given in Table 4 confirmed that MPAB shows  
354 competitive adsorption ability and affinity for MB in comparison to already reported  
355 adsorbents in literature. Moreover, the synthesized MPAB is a novel, competitive, and cost-  
356 effective adsorbent for MB adsorption. Therefore, it is recommended to use MPAB for removal  
357 of MB and other cationic dyes similar to MB.

358 **Table 4.**

### 359 **4. Conclusion**

360 In the present research work, MP waste was successfully encapsulated in alginate beads  
361 and used as an effective adsorbent for MB adsorption. The SEM and BET analysis confirmed  
362 that the beads are mesoporous in nature and have a porous surface. The FITR analysis  
363 confirmed that synthesized beads have nucleophilic sites on the surface which are capable of  
364 attracting MB molecules from aqueous phase. The adsorption study confirmed that MPAB  
365 composite has the potential to efficiently adsorb MB from aqueous solution. It has been  
366 concluded from the experimental results that MB adsorption significantly depends on initial  
367 pH of MB solution, contact time, initial MB concentration, and temperature. The adsorption  
368 capacity was found to increase with an increase in pH from acidic to basic conditions, contact  
369 time, and initial concentration of MB solution. Kinetic study confirmed that a PSO model well  
370 explained the adsorption of MB on the beads. Moreover, both Freundlich and Langmuir  
371 isotherms models described well the isotherm data of adsorption. Conclusively, we can claim  
372 that MPAB composite can be effectively applied as a low cost, potential, sustainable and  
373 environmentally friendly sorbent for the effective removal of MB and other cationic dyes.

### 374 **Acknowledgements**

375 The Deanship of Scientific Research (DSR) at King Abdulaziz University, Jeddah, Saudi  
376 Arabia funded this project, under grant no. (KEP-8-130-42).

377 **Conflict of interest:** We wish to confirm that no conflict of interest associated with this  
378 publication and the manuscript has been read and approved by all named authors.

### 379 **References**

- 380 [1] M. N. Chollom, "Treatment and reuse of reactive dye effluent from textile industry  
381 using membrane technology," Durban University of Technology, 2014.
- 382 [2] M. T. Yagub, T. K. Sen, S. Afroze, and H. M. Ang, "Dye and its removal from aqueous  
383 solution by adsorption: a review," *Advances in colloid and interface science*, vol. 209,  
384 pp. 172-184, 2014.
- 385 [3] K. C. Bedin, A. C. Martins, A. L. Cazetta, O. Pezoti, and V. C. Almeida, "KOH-  
386 activated carbon prepared from sucrose spherical carbon: Adsorption equilibrium,  
387 kinetic and thermodynamic studies for Methylene Blue removal," *Chemical  
388 Engineering Journal*, vol. 286, pp. 476-484, 2016.
- 389 [4] M. I. Khan, T. K. Min, K. Azizli, S. Sufian, H. Ullah, and Z. Man, "Effective removal  
390 of methylene blue from water using phosphoric acid based geopolymers: synthesis,  
391 characterizations and adsorption studies," *RSC Advances*, vol. 5, no. 75, pp. 61410-  
392 61420, 2015.
- 393 [5] J. Chang *et al.*, "Adsorption of methylene blue onto Fe<sub>3</sub>O<sub>4</sub>/activated montmorillonite  
394 nanocomposite," *Applied Clay Science*, vol. 119, pp. 132-140, 2016.
- 395 [6] S. Mashhadi, H. Javadian, M. Ghasemi, T. A. Saleh, and V. K. Gupta, "Microwave-  
396 induced H<sub>2</sub>SO<sub>4</sub> activation of activated carbon derived from rice agricultural wastes for  
397 sorption of methylene blue from aqueous solution," *Desalination and Water Treatment*,  
398 pp. 1-14, 2016.
- 399 [7] K. Y. Hor *et al.*, "Evaluation of physicochemical methods in enhancing the adsorption  
400 performance of natural zeolite as low-cost adsorbent of methylene blue dye from  
401 wastewater," *Journal of Cleaner Production*, vol. 118, pp. 197-209, 2016.
- 402 [8] Z. Li, Y. Yao, G. Wei, W. Jiang, Y. Wang, and L. Zhang, "Adsorption and heat-energy-  
403 aid desorption of cationic dye on a new thermo-sensitive adsorbent: Methyl  
404 cellulose/calcium alginate beads," *Polymer Engineering & Science*, vol. 56, no. 12, pp.  
405 1382-1389, 2016.
- 406 [9] K.-W. Jung, T.-U. Jeong, H.-J. Kang, and K.-H. Ahn, "Characteristics of biochar  
407 derived from marine macroalgae and fabrication of granular biochar by entrapment in  
408 calcium-alginate beads for phosphate removal from aqueous solution," *Bioresource  
409 technology*, vol. 211, pp. 108-116, 2016.
- 410 [10] A. L. Serpa, I. A. H. Schneider, and J. Rubio, "Adsorption onto fluidized powdered  
411 activated carbon flocs-PACF," *Environmental science & technology*, vol. 39, no. 3, pp.  
412 885-888, 2005.
- 413 [11] J.-S. Yang, Y.-J. Xie, and W. He, "Research progress on chemical modification of  
414 alginate: A review," *Carbohydrate polymers*, vol. 84, no. 1, pp. 33-39, 2011.
- 415 [12] A. F. Hassan, A. M. Abdel-Mohsen, and M. M. G. Fouda, "Comparative study of  
416 calcium alginate, activated carbon, and their composite beads on methylene blue  
417 adsorption," *Carbohydrate Polymers*, vol. 102, pp. 192-198, 2014.
- 418 [13] W. Khanday, M. Asif, and B. Hameed, "Cross-linked beads of activated oil palm ash  
419 zeolite/chitosan composite as a bio-adsorbent for the removal of methylene blue and  
420 acid blue 29 dyes," *International journal of biological macromolecules*, vol. 95, pp.  
421 895-902, 2017.
- 422 [14] C. Li, J. Lu, S. Li, Y. Tong, and B. Ye, "Synthesis of Magnetic Microspheres with  
423 Sodium Alginate and Activated Carbon for Removal of Methylene Blue," *Materials*,  
424 vol. 10, no. 1, p. 84, 2017.

- 425 [15] M. Hachi, A. Chergui, A. Selatnia, and H. Cabana, "Valorization of the spent biomass  
426 of *Pleurotus mutilus* immobilized as calcium alginate biobeads for methylene blue  
427 biosorption," *Environmental Processes*, vol. 3, no. 2, pp. 413-430, 2016.
- 428 [16] A. Nasrullah, A. Bhat, A. Naeem, M. H. Isa, and M. Danish, "High surface area  
429 mesoporous activated carbon-alginate beads for efficient removal of methylene blue,"  
430 *International journal of biological macromolecules*, vol. 107, pp. 1792-1799, 2018.
- 431 [17] B. Wang, B. Gao, A. R. Zimmerman, and X. Lee, "Impregnation of multiwall carbon  
432 nanotubes in alginate beads dramatically enhances their adsorptive ability to aqueous  
433 methylene blue," *Chemical Engineering Research and Design*, vol. 133, pp. 235-242,  
434 2018.
- 435 [18] W. Ahlawat, N. Kataraiia, N. Dilbaghi, A. A. Hassan, S. Kumar, and K.-H. Kim,  
436 "Carbonaceous nanomaterials as effective and efficient platforms for removal of dyes  
437 from aqueous systems," *Environmental Research*, p. 108904, 2019.
- 438 [19] N. Boukhalfa, M. Boutahala, N. Djebri, and A. Idris, "Kinetics, thermodynamics,  
439 equilibrium isotherms, and reusability studies of cationic dye adsorption by magnetic  
440 alginate/oxidized multiwalled carbon nanotubes composites," *International journal of  
441 biological macromolecules*, vol. 123, pp. 539-548, 2019.
- 442 [20] Y. Li *et al.*, "Methylene blue adsorption on graphene oxide/calcium alginate  
443 composites," *Carbohydrate polymers*, vol. 95, no. 1, pp. 501-507, 2013.
- 444 [21] G. Ohemeng-Boahen, D. D. Sewu, and S. H. Woo, "Preparation and characterization  
445 of alginate-kelp biochar composite hydrogel bead for dye removal," *Environmental  
446 Science and Pollution Research*, pp. 1-13, 2019.
- 447 [22] M. A. Khan *et al.*, "Adsorption of cobalt onto graphite nanocarbon-impregnated  
448 alginate beads: Equilibrium, kinetics, and thermodynamics studies," *Chemical  
449 Engineering Communications*, vol. 201, no. 3, pp. 403-418, 2014.
- 450 [23] V. Javanbakht and R. Shafiei, "Preparation and performance of Alginate/basil seed  
451 mucilage biocomposite for removal of eriochrome black T dye from aqueous solution,"  
452 *International journal of biological macromolecules*, 2019.
- 453 [24] N. Tahir, H. N. Bhatti, M. Iqbal, and S. Noreen, "Biopolymers composites with peanut  
454 hull waste biomass and application for Crystal Violet adsorption," *International journal  
455 of biological macromolecules*, vol. 94, pp. 210-220, 2017.
- 456 [25] L. Ai, M. Li, and L. Li, "Adsorption of methylene blue from aqueous solution with  
457 activated carbon/cobalt ferrite/alginate composite beads: kinetics, isotherms, and  
458 thermodynamics," *Journal of Chemical & Engineering Data*, vol. 56, no. 8, pp. 3475-  
459 3483, 2011.
- 460 [26] A. R. Garrity, G. A. Morton, and J. C. Morton, "Nutraceutical mangosteen  
461 composition," ed: Google Patents, 2004.
- 462 [27] Y. Chen, B. Huang, M. Huang, and B. Cai, "On the preparation and characterization of  
463 activated carbon from mangosteen shell," *Journal of the Taiwan Institute of Chemical  
464 Engineers*, vol. 42, no. 5, pp. 837-842, 2011.
- 465 [28] S. d. Malaysia. (2016). *Mangosteen production in Malaysia*. Available:  
466 <https://newss.statistics.gov.my/newss-portalx/ep/epProductFreeDownload>
- 467 [29] A. Nasrullah *et al.*, "Mangosteen peel waste as a sustainable precursor for high surface  
468 area mesoporous activated carbon: Characterization and application for methylene blue  
469 removal," vol. 211, pp. 1190-1200, 2019.

- 470 [30] N. Asma *et al.*, "Efficient removal of methylene blue dye using mangosteen peel waste:  
471 kinetics, isotherms and artificial neural network (ANN) modeling," vol. 86, pp. 191-  
472 202, 2017.
- 473 [31] C. Saucier *et al.*, "Microwave-assisted activated carbon from cocoa shell as adsorbent  
474 for removal of sodium diclofenac and nimesulide from aqueous effluents," *Journal of*  
475 *hazardous materials*, vol. 289, pp. 18-27, 2015.
- 476 [32] S. Lagergren, "About the theory of so-called adsorption of soluble substances," 1898.
- 477 [33] G. Blanchard, M. Maunaye, and G. Martin, "Removal of heavy metals from waters by  
478 means of natural zeolites," *Water research*, vol. 18, no. 12, pp. 1501-1507, 1984.
- 479 [34] I. Langmuir, "The constitution and fundamental properties of solids and liquids. 11.  
480 Liquids," *J Am Chem Soc*, vol. 3, no. 9, pp. 1848-1906, 1917.
- 481 [35] H. Freundlich, "Over the adsorption in solution," *J. Phys. Chem*, vol. 57, no. 385, p.  
482 e470, 1906.
- 483 [36] M. Temkin and V. Pyzhev, "Kinetics of ammonia synthesis on promoted iron  
484 catalysts," *Acta physiochim. URSS*, vol. 12, no. 3, pp. 217-222, 1940.
- 485 [37] W. D. Harkins and G. Jura, "Surfaces of solids. XIII. A vapor adsorption method for  
486 the determination of the area of a solid without the assumption of a molecular area, and  
487 the areas occupied by nitrogen and other molecules on the surface of a solid," *Journal*  
488 *of the American Chemical Society*, vol. 66, no. 8, pp. 1366-1373, 1944.
- 489 [38] A. Hassan, A. Abdel-Mohsen, and M. M. Fouda, "Comparative study of calcium  
490 alginate, activated carbon, and their composite beads on methylene blue adsorption,"  
491 *Carbohydrate polymers*, vol. 102, pp. 192-198, 2014.
- 492 [39] A. Benhouria, M. A. Islam, H. Zaghouane-Boudiaf, M. Boutahala, and B. Hameed,  
493 "Calcium alginate–bentonite–activated carbon composite beads as highly effective  
494 adsorbent for methylene blue," *Chemical Engineering Journal*, vol. 270, pp. 621-630,  
495 2015.
- 496 [40] Y. Liu, Y. Zheng, and A. Wang, "Enhanced adsorption of Methylene Blue from  
497 aqueous solution by chitosan-g-poly (acrylic acid)/vermiculite hydrogel composites,"  
498 *Journal of environmental Sciences*, vol. 22, no. 4, pp. 486-493, 2010.
- 499 [41] M. Auta and B. H. Hameed, "Chitosan–clay composite as highly effective and low-cost  
500 adsorbent for batch and fixed-bed adsorption of methylene blue," *Chemical*  
501 *Engineering Journal*, vol. 237, pp. 352-361, 2014/02/01/ 2014.
- 502 [42] X. Qiao, S. Liao, C. You, and R. Chen, "Phosphorus and nitrogen dual doped and  
503 simultaneously reduced graphene oxide with high surface area as efficient metal-free  
504 electrocatalyst for oxygen reduction," *Catalysts*, vol. 5, no. 2, pp. 981-991, 2015.
- 505 [43] D. Everett, "Manual of symbols and terminology for physicochemical quantities and  
506 units, appendix II: Definitions, terminology and symbols in colloid and surface  
507 chemistry," *Pure and Applied Chemistry*, vol. 31, no. 4, pp. 577-638, 1972.
- 508 [44] A. Nasrullah *et al.*, "Calligonum polygonoides biomass as a low-cost adsorbent: surface  
509 characterization and methylene blue adsorption characteristics," *Desalination and*  
510 *Water Treatment*, no. ahead-of-print, pp. 1-13, 2015.
- 511 [45] L. Huang, Y. Chen, G. Liu, S. Li, Y. Liu, and X. Gao, "Non-isothermal pyrolysis  
512 characteristics of giant reed (*Arundo donax* L.) using thermogravimetric analysis,"  
513 *Energy*, 2015.

- 514 [46] W. M. Algothmi, N. M. Bandaru, Y. Yu, J. G. Shapter, and A. V. Ellis, "Alginate–  
515 graphene oxide hybrid gel beads: an efficient copper adsorbent material," *Journal of*  
516 *colloid and interface science*, vol. 397, pp. 32-38, 2013.
- 517 [47] X. Vecino, R. Devesa-Rey, J. Cruz, and A. Moldes, "Study of the physical properties  
518 of calcium alginate hydrogel beads containing vineyard pruning waste for dye  
519 removal," *Carbohydrate polymers*, vol. 115, pp. 129-138, 2015.
- 520 [48] İ. Sargin, G. Arslan, and M. Kaya, "Microfungal spores (*Ustilago maydis* and *U.*  
521 *digitariae*) immobilised chitosan microcapsules for heavy metal removal,"  
522 *Carbohydrate polymers*, vol. 138, pp. 201-209, 2016.
- 523 [49] A. A. Oladipo and M. Gazi, "Enhanced removal of crystal violet by low cost  
524 alginate/acid activated bentonite composite beads: Optimization and modelling using  
525 non-linear regression technique," *Journal of Water Process Engineering*, vol. 2, pp. 43-  
526 52, 2014.
- 527 [50] Y. Zhuang, F. Yu, J. Chen, and J. Ma, "Batch and column adsorption of methylene blue  
528 by graphene/alginate nanocomposite: Comparison of single-network and double-  
529 network hydrogels," *Journal of Environmental Chemical Engineering*, vol. 4, no. 1, pp.  
530 147-156, 2016.
- 531 [51] A. Nasrullah *et al.*, "Mangosteen peel waste as a sustainable precursor for high surface  
532 area mesoporous activated carbon: Characterization and application for methylene blue  
533 removal," *Journal of Cleaner Production*, vol. 211, pp. 1190-1200, 2019.
- 534 [52] T. Sheela and Y. A. Nayaka, "Kinetics and thermodynamics of cadmium and lead ions  
535 adsorption on NiO nanoparticles," *Chemical engineering journal*, vol. 191, pp. 123-  
536 131, 2012.
- 537 [53] S. Lapwanit, T. Sooksimuang, and T. Trakulsujaritchok, "Adsorptive removal of  
538 cationic methylene blue dye by kappa-carrageenan/poly (glycidyl methacrylate)  
539 hydrogel beads: Preparation and characterization," *Journal of environmental chemical*  
540 *engineering*, vol. 6, no. 5, pp. 6221-6230, 2018.
- 541 [54] L. Liu, Y. Wan, Y. Xie, R. Zhai, B. Zhang, and J. Liu, "The removal of dye from  
542 aqueous solution using alginate-halloysite nanotube beads," *Chemical engineering*  
543 *journal*, vol. 187, pp. 210-216, 2012.
- 544 [55] Y. Li, S.-j. Liu, F.-m. Chen, and J.-e. Zuo, "High-Strength Apatite/Attapulgitite/Alginate  
545 Composite Hydrogel for Effective Adsorption of Methylene Blue from Aqueous  
546 Solution," *Journal of Chemical & Engineering Data*, 2019.
- 547 [56] H. W. Kwak, Y. Hong, M. E. Lee, and H.-J. Jin, "Sericin-derived activated carbon-  
548 loaded alginate bead: An effective and recyclable natural polymer-based adsorbent for  
549 methylene blue removal," *International journal of biological macromolecules*, vol.  
550 120, pp. 906-914, 2018.
- 551 [57] A. Saha, V. Tripathy, B. Basak, and J. Kumar, "Entrapment of distilled palmarosa  
552 (*cymbopogon martinii*) wastes in alginate beads for adsorptive removal of methylene  
553 blue from aqueous solution," *Environmental Progress & Sustainable Energy*, vol. 37,  
554 no. 6, pp. 1942-1953, 2018.
- 555 [58] N. Mohammed, N. Grishkewich, R. M. Berry, and K. C. Tam, "Cellulose nanocrystal–  
556 alginate hydrogel beads as novel adsorbents for organic dyes in aqueous solutions,"  
557 *Cellulose*, vol. 22, no. 6, pp. 3725-3738, 2015.

- 558 [59] Y.-y. Pei, Z.-y. Xiao, S.-r. Zhai, and B. Zhai, "Biomass-based carbon beads with a  
559 tailored hierarchical structure and surface chemistry for efficient batch and column  
560 uptake of methylene blue," *Research on Chemical Intermediates*, vol. 44, no. 4, pp.  
561 2867-2887, 2018.
- 562 [60] Ş. Parlayıcı, "Alginate-coated perlite beads for the efficient removal of methylene blue,  
563 malachite green, and methyl violet from aqueous solutions: kinetic, thermodynamic,  
564 and equilibrium studies," *Journal of Analytical Science and Technology*, vol. 10, no. 1,  
565 p. 4, 2019.
- 566 [61] Y. Li *et al.*, "Methylene blue adsorption on graphene oxide/calcium alginate  
567 composites," vol. 95, no. 1, pp. 501-507, 2013.
- 568 [62] S. Lapwanit, T. Sooksimuang, and T. J. J. o. e. c. e. Trakulsujaritchok, "Adsorptive  
569 removal of cationic methylene blue dye by kappa-carrageenan/poly (glycidyl  
570 methacrylate) hydrogel beads: Preparation and characterization," vol. 6, no. 5, pp.  
571 6221-6230, 2018.
- 572 [63] L. Liu, Y. Wan, Y. Xie, R. Zhai, B. Zhang, and J. J. C. E. J. Liu, "The removal of dye  
573 from aqueous solution using alginate-halloysite nanotube beads," vol. 187, pp. 210-  
574 216, 2012.
- 575 [64] Y. Li, S.-j. Liu, F.-m. Chen, J.-e. J. J. o. C. Zuo, and E. Data, "High-Strength  
576 Apatite/Attapulgitite/Alginate Composite Hydrogel for Effective Adsorption of  
577 Methylene Blue from Aqueous Solution," 2019.
- 578 [65] H. W. Kwak, Y. Hong, M. E. Lee, and H.-J. J. I. j. o. b. m. Jin, "Sericin-derived  
579 activated carbon-loaded alginate bead: An effective and recyclable natural polymer-  
580 based adsorbent for methylene blue removal," vol. 120, pp. 906-914, 2018.
- 581

## LIST OF TABLES

**Table 1.** Pseudo first and pseudo second order model parameters for adsorption of MB on MPAB

C <sub>o</sub>	Pseudo-first order kinetic				Pseudo-second order kinetic		
	q <sub>exp</sub> (mg.g <sup>-1</sup> )	q <sub>cal</sub> (mg.g <sup>-1</sup> )	k <sub>1</sub> (min <sup>-1</sup> )	R <sup>2</sup>	q <sub>cal</sub> (mg.g <sup>-1</sup> )	k <sub>2</sub> (g.min.mg <sup>-1</sup> )	R <sup>2</sup>
20	38.28	41.30	0.0069	0.960	39.88	0.000598	0.997
40	75.98	172.99	0.0110	0.937	80.97	0.000197	0.995
60	113.49	175.81	0.0072	0.925	124.68	7.88E-05	0.992
80	149.55	213.80	0.0068	0.896	161.81	7.18E-05	0.995
100	184.938	152.63	0.0045	0.960	197.62	5.80E-05	0.995

**Table 2.** Langmuir, Freundlich, Harkins Jura and Tempkin isotherms model parameters for adsorption of MB on MPAB.

Type	Linear form	Plot	parameters
Langmuir	$\frac{C_e}{q_e} = \frac{1}{bQ_o} + \frac{C_e}{Q_o}$	$\frac{C_e}{q_e}$ vs C <sub>e</sub>	Q <sub>o</sub> (mg/g) = 373.00 b (L/mg) = 0.131. R <sup>2</sup> = 0.995
Freundlich	$\ln q_e = \ln K_F + \frac{1}{n} \ln C_e$	ln q <sub>e</sub> vs C <sub>e</sub>	n = 1.35 K <sub>F</sub> (mg/g) = 44.69 R <sup>2</sup> = 0.989
Tempkin	$q_e = B \ln A + B \ln C_e$	q <sub>e</sub> vs ln C <sub>e</sub>	B = 68.648 A = 1.712 R <sup>2</sup> = 0.934
Harkins Jura	$\frac{1}{q_e^2} = \frac{B}{A} - \frac{1}{A} \log C_e$	$\frac{1}{q_e^2}$ vs log C <sub>e</sub>	B = -0.759 A = -1466.05 R <sup>2</sup> = 0.764

**Table 3.** Thermodynamic parameters for adsorption of MB on MPAB.

T (K)	$\Delta G^\circ$ (kJ/mol)	$\Delta H^\circ$ (kJ/mol)	$\Delta S^\circ$ (J/mol.K)
298	-7.93		
303	-7.36		
313	-7.15	-31.48	-77.47
323	-6.08		
333	-5.06		

**Table. 4** Comparison of adsorption capacity of MPAB with reported alginate beads

Adsorbents	q (mg/g)	Reference
GO/Ca-alginate composites	181.81	[19]
Kappa-carrageenan/poly(glycidylmethacrylate) hydrogel beads	166.62	[54]
Alginate-halloysite nanotube beads	250	[55]
Apatite/Attapulgitte/Alginate Composite Hydrogel	244.6	[56]
Sericin-derived activated carbon (S-AC)/Alg beads	502.5	[57]
Palmarosa entrapped in alginate beads	6.45	[50]
Cellulose nanocrystal–alginate hydrogel beads	256.41	[51]
Alginate-derived carbon beads	397.9	[52]
Alginate-coated perlite beads	104.	[53]
Pleurotus mutilus Immobilized as Calcium Alginate Biobeads	23	[15]
Mp-alginate beads	373	Present study

## LIST OF FIGURES



**Fig. 1.** Typical photograph of MPAB.

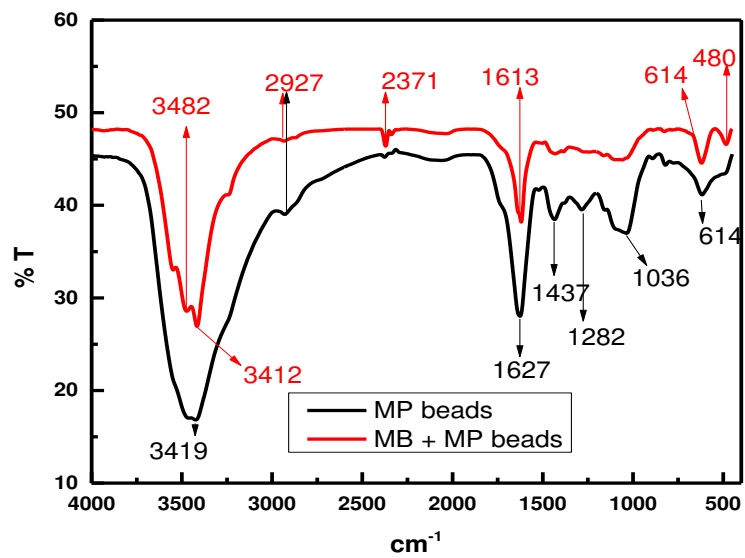


**Fig. 2.** FTIR spectra of MPAB before and after MB adsorption.

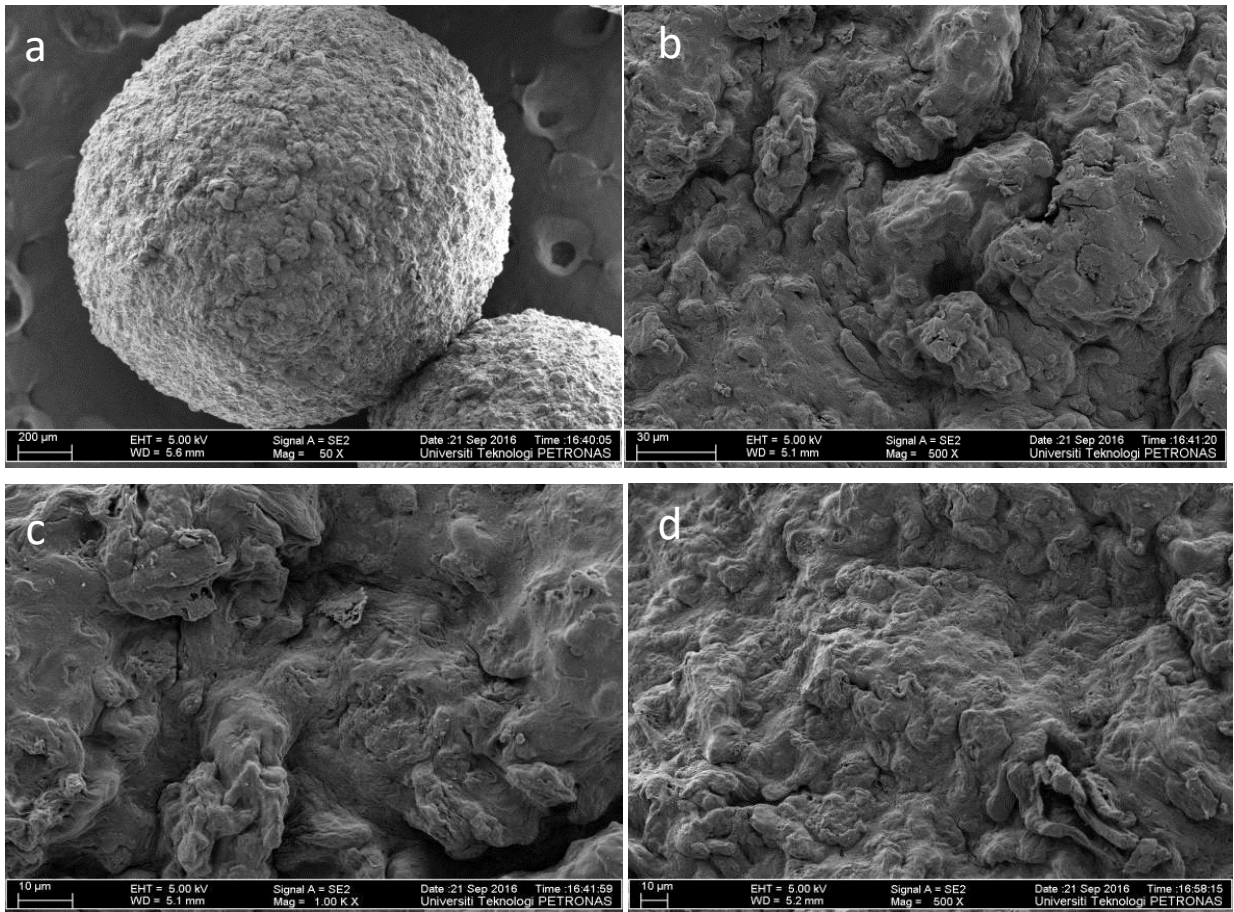


**Fig. 3.** SEM photographs analysis of MPAB.

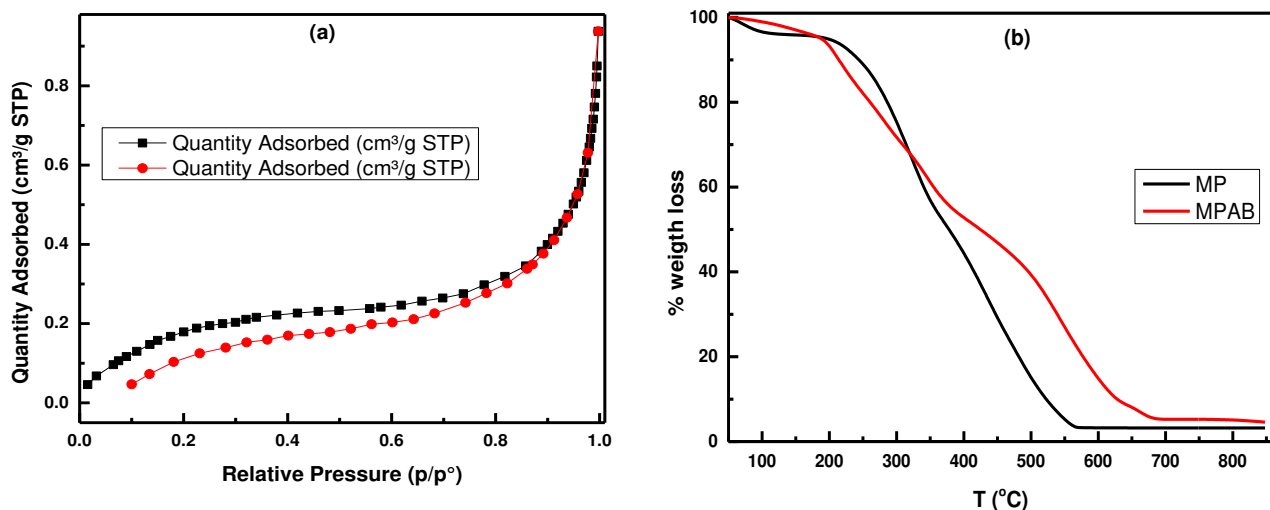


**Fig. 4.** (a) N<sub>2</sub> adsorption–desorption isotherms and (b) Thermal degradation of MPAB

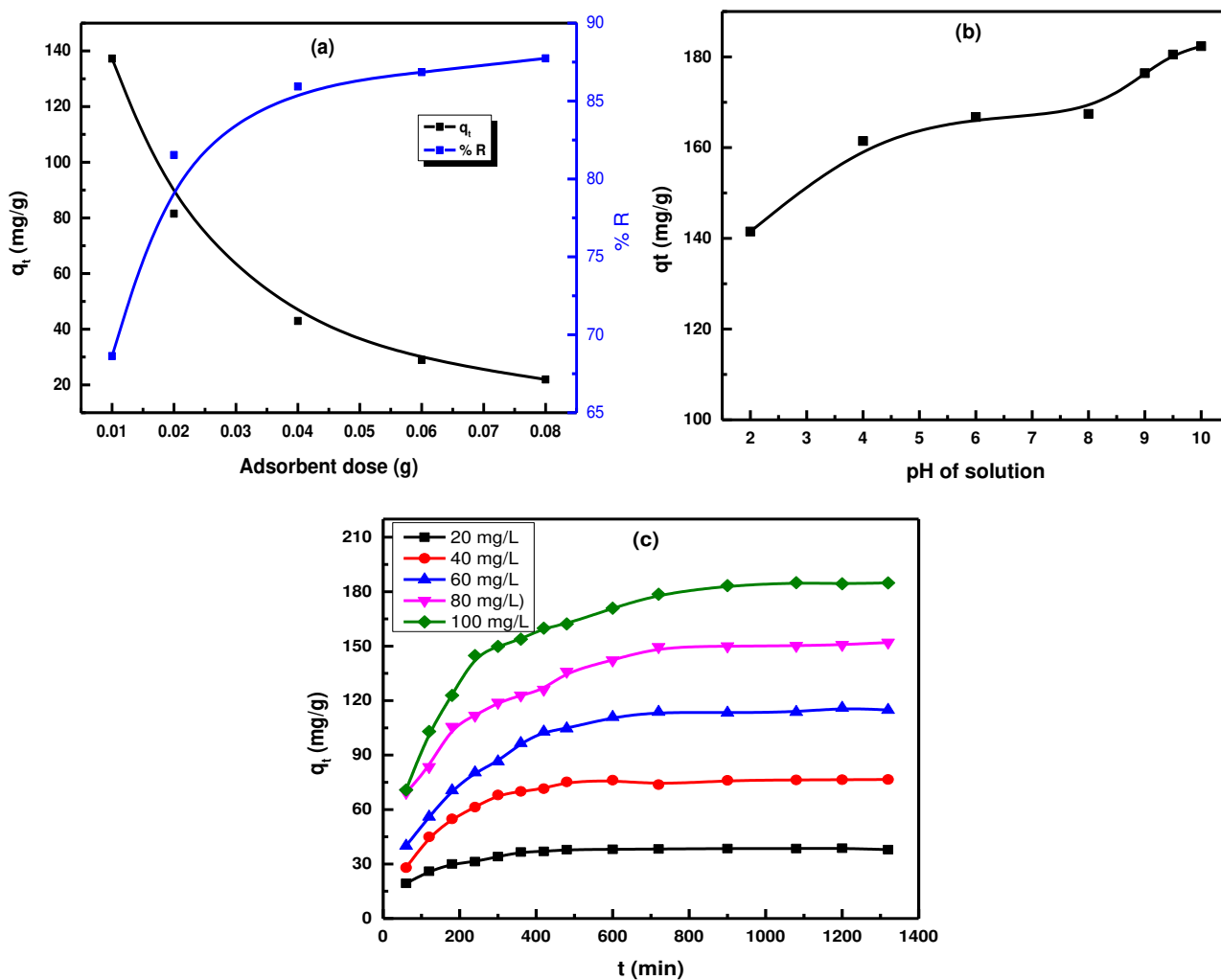


**Fig. 5.** Effect of (a) adsorbent dose and (b) initial pH and contact time on MB adsorption on MPAB.

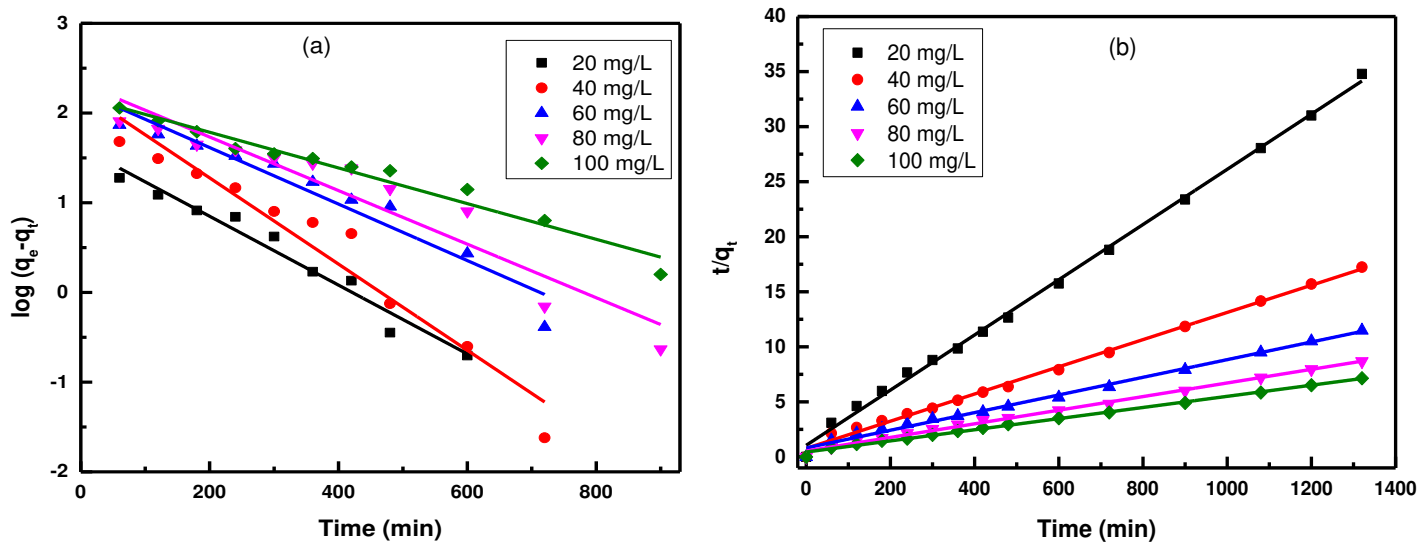


**Fig. 6.** (a) Pseudo first and (b) pseudo second order kinetic plots for adsorption of MB on MPAB.

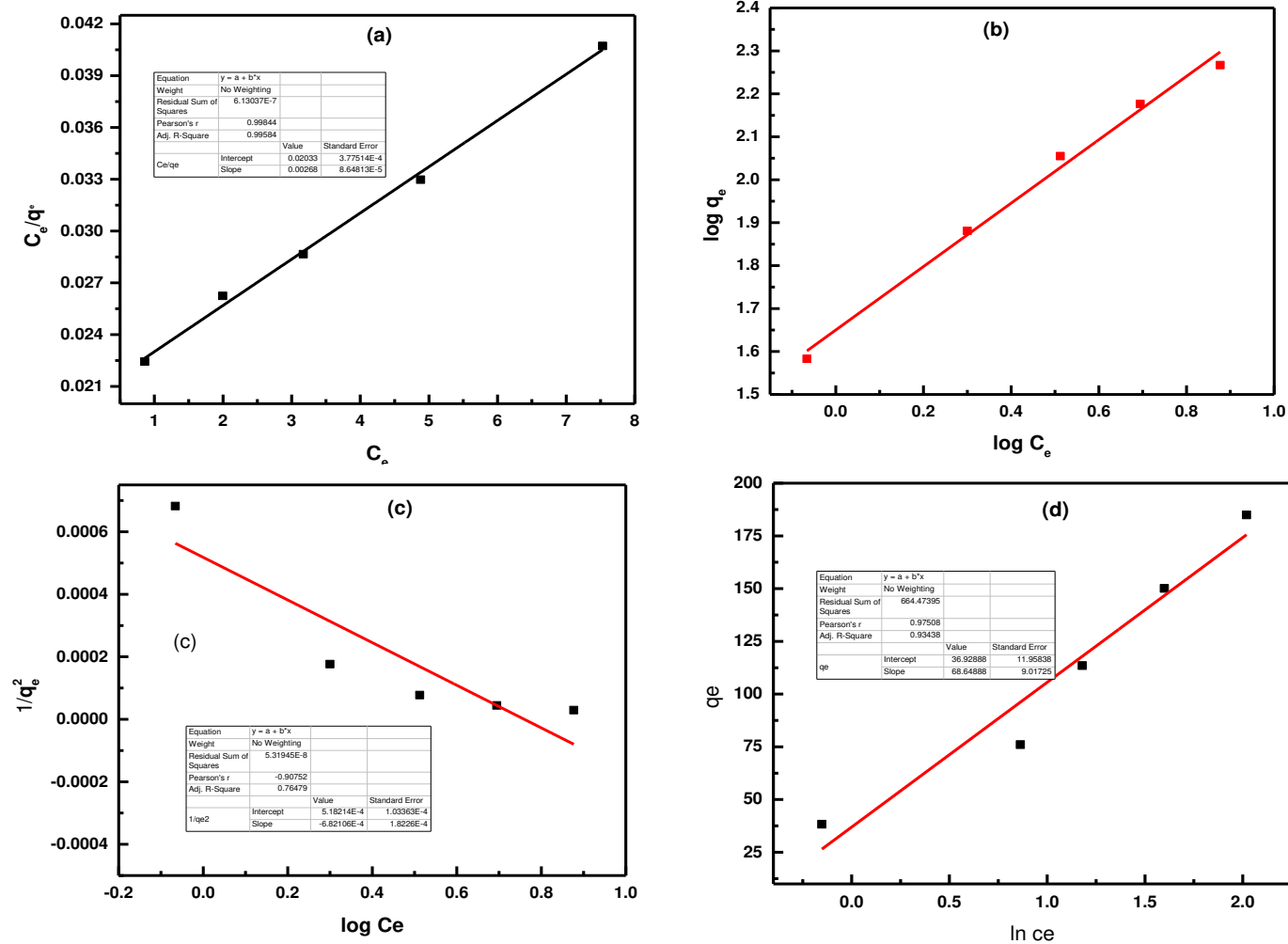


**Fig. 7.** (a) Langmuir, (b) Freundlich, (c) Harkins-Jura and (d) Temppkin isotherms model for MB adsorption on MPAB.

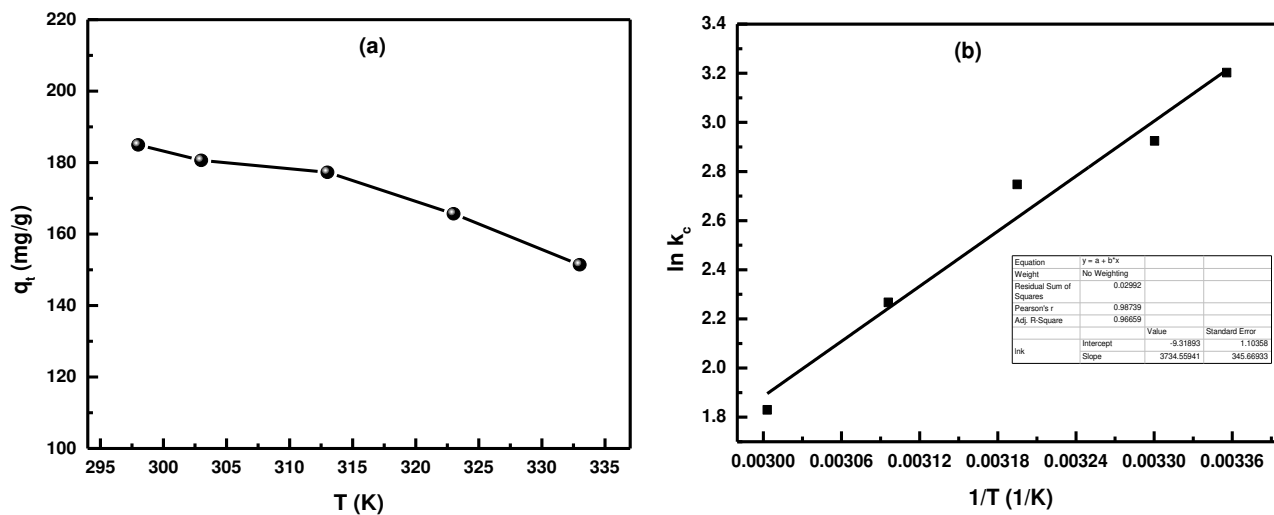


**Fig. 8.** Effect of temperature on MB adsorption and (b) Arrhenius plot for MB adsorption on MPAB

## Supplementary Files

This is a list of supplementary files associated with this preprint. Click to download.

- [SupplementaryMaterial.docx](#)